Available online at www.sciencedirect.com

ScienceDirect

Nuclear Instruments and Methods in Physics Research A 568 (2006) 537–542

NUCLEAR INSTRUMENTS & METHODS IN PHYSICS RESEARCH Section A

www.elsevier.com/locate/nima

Operation of the MAMI accelerator with a Wien filter based spin rotation system

V. Tioukine*, K. Aulenbacher

Institut für Kernphysik, Johannes-Gutenberg Universität Mainz, J.-J. Becherweg 45, D-55099 Mainz, Germany

Received 7 October 2005; received in revised form 9 August 2006; accepted 10 August 2006
Available online 5 September 2006

Abstract

A compact spin rotation system based on a Wien filter has been installed at the Mainz microtron accelerator (MAMI). Under operation with varying spin rotation angles a significant change of focal length together with a shift of the central beam trajectory is expected. We demonstrate that these effects can be kept under control. As a consequence operation with spin rotation angles between 0° and $\pm 90^\circ$ has been achieved without compromising the beam quality and operational stability of MAMI.

PACS: 29.27.−a; 29.27.Eg; 29.27.Hj

Keywords: Accelerator; Wien filter; Spin

1. Introduction

The Mainz microtron accelerator (MAMI) provides acceleration of spin-polarized electrons in a 3-stage microtron cascade [1,2]. Nowadays the major part of run time at MAMI is used for spin-polarized electron scattering. These experiments are dedicated to, e.g., the determination of nucleon form factors [3], test of GDH sum rule [4] and precise measurement of parity violation [5].

The source produces longitudinally polarized electrons, that is the polarization vector is oriented along the particle velocity. The final beam energy for the experiments ranges between 180 and 855 MeV and will rise to 1500 MeV with the upcoming fourth microtron stage, MAMI-C. The spin motion in an electromagnetic field is described by the Thomas-BMT equation [6,7]. When as in MAMI the accelerating electric field is parallel to the particle velocity and the guiding magnetic field is perpendicular to it, the spin of the reference particle precesses around the magnetic field with angular frequency

$$\omega_s = (1 + a\gamma)\omega_c \tag{1}$$

where $\omega_c = eB/m\gamma$ (e, $m =$ electron charge and rest mass, $\gamma = 1 + T/m$ with $T =$ kinetic energy) is the cyclotron frequency and $a = (g-2)/2 \approx 1/862$ is the electron anomalous magnetic moment. As ω_s is not an integer multiple of ω_c, the final orientation of the polarization of the extracted beam at the experiment location is in general not parallel to the particle velocity. The spin rotation system originally designed [8] for controlling the spin direction at the experiment location could not be installed due to lack of space. The solution adopted of tuning the accelerator final energy was not fully satisfactory for experiment below 500 MeV and would have required additional investment costs for MAMI-C [9].

A Wien filter has been therefore installed in the injection beam line at a kinetic energy of 100 keV. This compact device allows to choose the desired spin orientation for all envisaged experiments with energies ranging from 3.5 MeV (the operating energy of the recently installed Mott polarimeter) up to 1500 MeV.

Our Wien filter is a copy from a design that was built at the Stanford linear accelerator [10]. Similar devices are presently

*Corresponding author. Tel.: +49 6131 3922934; fax: +49 6131 3922964.
E-mail address: tioukine@kph.uni-mainz.de (V. Tioukine).

0168-9002/$ - see front matter
doi:10.1016/j.nima.2006.08.022

in operation at JLAB and MIT/Bates [11]. It seems to us that details of its electron optical properties have not been published. Since the MAMI accelerator has more stringent requirements on transverse emittance and matching of the beam phase space ellipse—at least compared to the pulsed machines—a closer look into these subjects seemed necessary.

The basic electron optical principles and the set up of the Wien-filter system used in this investigation are described in the next section. Section three presents experimental observations and results that have been obtained after the installation at MAMI. The performance of the system in operation for experiments at MAMI is discussed in the final section.

2. Principle of operation

2.1. Wien-filter setup

A view of the installation is presented in Fig. 2. The filter is installed on the injection axis of the MAMI preaccelerator. An important detail is that it is located between two circular tungsten collimators (input/output collimator) of 2.5 mm diameter. The reference beam trajectory coincides with the centers of the collimators. The available space of about 90 cm between the collimators allowed for the installation of the filter, a view screen for beam diagnostics and of an additional quadrupole doublet. The geometrical centers of these additional devices are also aligned with the reference trajectory.

A Wien-filter spin-rotator consists of homogenous electric ($\vec{E}$) and magnetic fields ($\vec{B}$) which are perpendicular to each other and transverse to the direction of the particle motion (with velocity $\vec{v}$). In order to achieve the condition of no deflection from the reference beam trajectory the vectors of fields and velocity must fulfill the force-equilibrium condition

$$\vec{B} \times \vec{v} = \vec{E} \qquad (2)$$

A cross-section of the filter can be found in Fig. 1. The electric field is produced by two electrostatic condenser plates. Symmetrical supply of the two plates ensures that the 0-V equipotential coincides with the symmetry axis of the condenser. The magnetic field is produced by a magnet of the 'window frame' type.

2.2. Basic parameters

The polarized source at MAMI produces longitudinally polarized electrons. According to the Thomas-BMT equation the spin is rotated by the Wien filter in the plane perpendicular to $\vec{B}$. In order to achieve the demanded angle Θ of spin rotation without causing a beam deflection, the relationship $\vec{B} \times \vec{v} = \vec{E}$ must be fulfilled while varying the absolute value of the fields. Assuming force equilibrium (2) and $a \ll 1$ the Thomas-BMT equation leads to the following relation between $\vec{B}$ and Θ:

$$B = mc\gamma^2\beta\Theta/eL \qquad (3)$$

The effective field length L is 0.32 m. For our case the values of the relativistic parameters are $\gamma = 1.1953$ and $\beta = v/c = 0.5478$. Consequently, a $\pi/2$ spin rotation

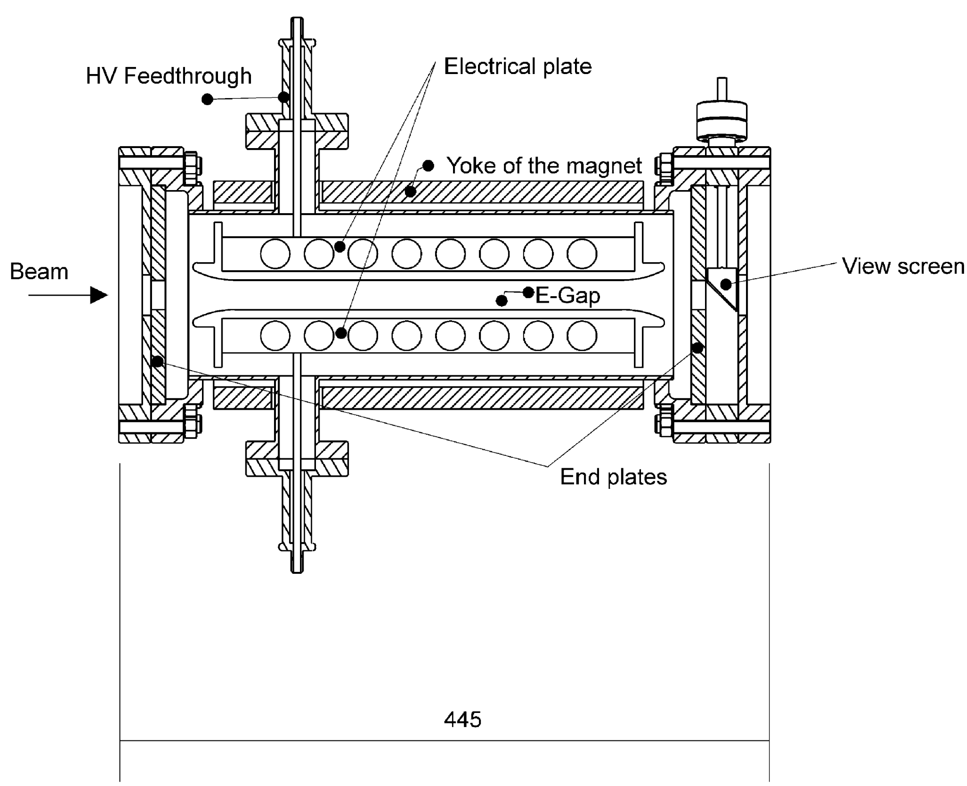

Fig. 1. Wien-filter cross-section, length is in mm.

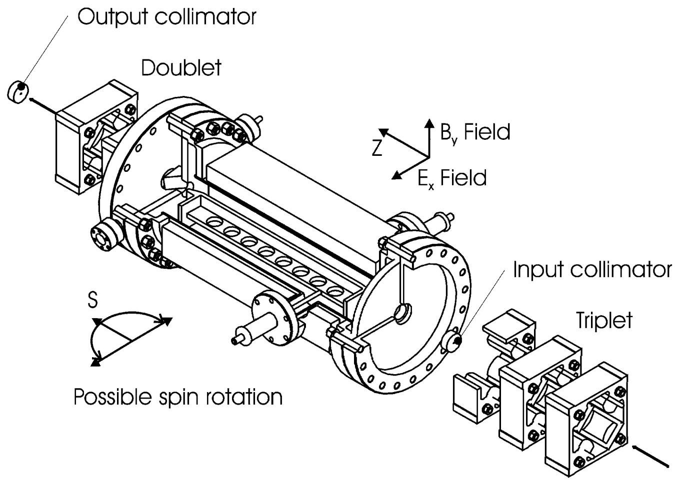

Fig. 2. Wien-filter installation in the 100 keV injection beam line. Magnet yoke and other parts are partially cut away for better visibility.

requires the following field strengths (coordinates are indicated in Fig. 2):

$$B_y = 65.63\,\mathrm{G}$$

$$E_x = 1.0788\,\mathrm{MV/m}$$

The high voltage capabilities of the filter where tested for a field of 1.25 MV/m (25 kV over the 2 cm gap of the condenser) without problems. In practice it is therefore possible to provide reliable spin rotation for an angular range of $\pm\pi/2$, the negative values are easily achieved by reversing the field directions. In addition, the spin orientation may be flipped by reversing the source laser helicity [2]. As a result any spin orientation in the machine plane may be obtained. Finally, by adding a longitudinal magnetic field behind the Wien filter it would be possible to introduce an orthogonal axis of rotation of the spin whose direction could therefore span the whole space. We have not investigated this option yet since no demands have been raised by the experimenters so far.

3. Electron optical properties and experimental observations

3.1. Variable focusing strength

When Eq. (2) is fulfilled, the transport matrix for the horizontal motion is, in the hard edge approximation, given by [12]

$$T = \begin{pmatrix} \cos(L/R) & R\sin(L/R) & -R(1-\cos(L/R)) \\ -R^{-1}\sin(L/R) & \cos(L/R) & -\sin(L/R) \\ 0 & 0 & 1 \end{pmatrix} \tag{4}$$

with $R \equiv \gamma m v/eB$. In our case, making use of Eq. (3), is $R = L/\gamma\Theta$.

In the ideal case there is instead no force in the vertical plane but for extended fringe fields a defocusing in the vertical plane exists which is proportional to R^{-2} [12].

The matrix elements T_{13} and T_{23} in Eq. (4) can be neglected for our case since the input beam is nearly monoenergetic with $\mathrm{d}v/v \approx 10^{-5}$. The transverse coordinates are affected by the other matrix elements. With Θ varying between 0 and $\pi/2$, the matrix element T_{21}, for instance, varies between 0 and $5.5\,\mathrm{m}^{-1}$. This raises the question whether the beam phase space ellipse will stay matched to the accelerator acceptance throughout the tuning range. The problem is considerably reduced by the fact that the filter is installed at a point where the injection system provides a focus in order to obtain the best possible transmission through the input and output collimator. Therefore the influence of T_{21} on the beam parameters is minimized. This assumption was confirmed by computer simulations which were performed prior to the installation at MAMI [9].

3.2. Emittance measurements

Fig. 3 shows the result of emittance measurements for different settings of the spin rotation angle. The method applied was measuring the horizontal and vertical beam diameters with a wire scanner while varying the current in a compensated solenoid lens in front of it. The compensated solenoid consists of two equal coils with opposite integrated strength in the second coil, a so-called anti-solenoid. Using such a device avoids the unwanted rotation of transverse coordinates [13,14]. In addition, the overall precession of the polarisation vector in the solenoid is proportional to [15]

$$\Theta = \int B_z \mathrm{d}z \tag{5}$$

and vanishes. The transport matrix elements of the system consisting of the compensated solenoid and the drift towards the scanner are varied with the current which allows to extract the phase space ellipse from the beam width measurements [16].

A change of the orientation of the beam phase space ellipse is visible in both the horizontal and the vertical plane. We believe that the vertical change is a manifestation of the effect of the extended fringe fields mentioned above.

The phase space ellipse variations cause no problems in practical operation: We have observed negligible (between 0.5% and 3%) beam losses at the output collimator while tuning the spin rotation angle from 0 to $\pi/2$. No change in the loss rate during acceleration was observed, which indicates that the matching conditions are not compromised. In addition, operation of the spin rotator did not cause a noticeable effect on the beam parameters at the experiments for the whole tuning range.

In principle it is possible to compensate the variations of the beam phase space ellipse by changing the setting of the five quadrupoles depicted in Fig. 2, as was outlined in

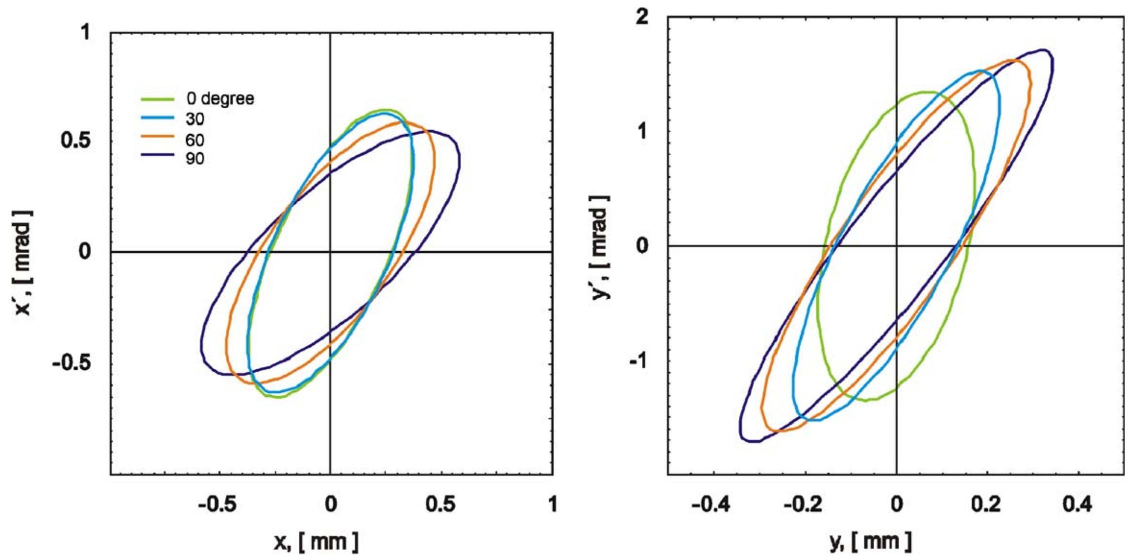

Fig. 3. Experimentally observed variation of beam phase space ellipse orientation in the horizontal (x, x'-) and in the vertical (y, y'-) plane.

Ref. [9]. However, because of the absence of problems implied by these effects we have not yet investigated this option.

3.3. Shift of central beam trajectory

When considering a fringe field of finite dimension, in addition to the optic perturbation mentioned above, the device can introduce a distortion of the horizontal beam trajectory, unless the length of the magnetic and electric fringe fields are equal. In our case the electrical field plate arrangement leads to a smaller 'electrical gap' if compared with the magnetic gap since the condenser plates have to be installed inside the aperture of the magnet (see Fig. 1). Therefore the electrical fringe field has a shorter extension compared to the magnetic one. This is demonstrated by a field calculation which we performed with the help of the TOSCA and CPO-3d software packages. The result for $E_x/E_{x,0}$ and $B_y/B_{y,0}$ on the reference line is presented in Fig. 4 under the assumption that the fields inside the filter ($E_{x,0}$, $B_{y,0}$) are adjusted to fulfill Eq. (2). As could be expected from the geometric consideration above the ratio E/B is $<v$ in the outer fringe field whereas it is $>v$ for positions close to the homogeneous part of the field. Therefore a particle which is entering the system on the reference beam trajectory will first be deflected away from it in the outer fringe field. This angular deflection ('kick') will be partially compensated by the inner part. In general a shift in both position and angle of the beam has to be expected. Salomaa and Enge [12] give an expression for the trajectory shift under the assumption that the angular kick vanishes due to equal effective lengths of electric and magnetic fields. In terms of spin rotation angle, the trajectory shift is given by

$$\Delta x = I_1(D_m^2 - D_e^2)\gamma\Theta/L \tag{6}$$

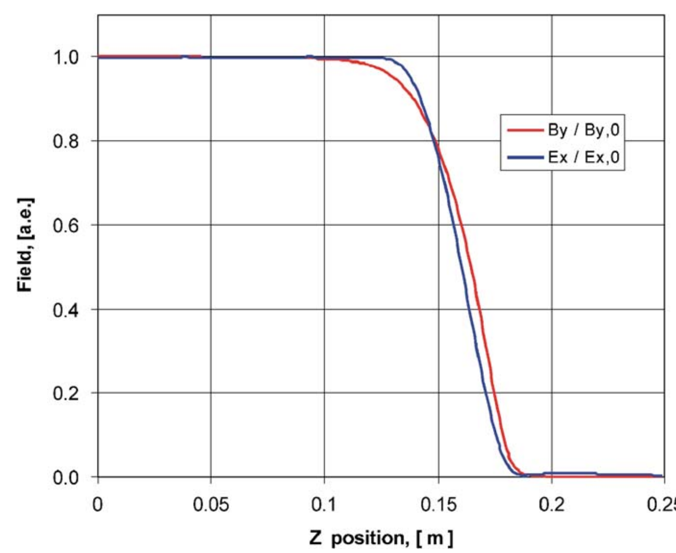

Fig. 4. Computed E- and B-field variations on the z-axis.

In our case the electrical and magnetic gap width are $D_e = 4$ cm and $D_m = 6$ cm. I_1 is a numerical constant which has to be obtained from the actual shape of the fringe field. For our case the evaluation of the fringe field integral leads to the prediction that the maximum Δx is of the order of 1–2 mm. The limitation to this rather small value is mostly due to two effects. First the widening of the electrical gap near the edge of the condenser (which is also helpful to reduce the field strength at the edge of the condenser plates) decreases the value of the difference in Eq. 5. The other is the geometrical confinement of both fringe fields by the end plates (see Fig. 2) which reduces the value of I_1.

By performing three dimensional particle tracking through the actual field geometry of the filter we found that the real behavior of the beam should be more complex, especially that the angular kick after the filter should not be zero, but a few milliradians.

The actual trajectory distortion produced by the device can be easily observed on the view screen behind the filter. First the beam is carefully adjusted onto the reference axis with no fields in the Wien filter. When turning on the fields to their nominal values for the maximum required spin rotation angle, namely $\pi/2$, we observe a change of the beam trajectory on the Wien-filter view screen of 3 mm in the horizontal direction. We also observe an additional kick of 2–3 mrad at the output of the filter. These observations are in qualitative agreement with our computer simulations, at least for the horizontal plane. In addition we see a small vertical movement of about 1 mm, which is probably due to a misalignment of the injected beam with respect to the reference axis. In operation the beam is readjusted to the reference axis by the following procedure: a change of E_x (typically by a few 10^{-3}) serves as horizontal steering mechanism whereas vertical steering is achieved by a corrector magnet (not shown in Fig. 2) that is placed directly downstream from the input collimator.

These changes allow us to vary the output beam direction so that the transmission through the output collimator gets restored. The reference position on the view screen cannot be conserved simultaneously because this would require using an additional steerer in the vicinity of the screen to compensate for the angular kick. Such a steerer has not been installed due to space restrictions. The deviations from the reference beam trajectory are <3.5 mm which can be tolerated because of the small beam envelope and large aperture (>20 mm). The remaining angular deviation is then compensated by steerers located behind the output collimator.

3.4. Horizontal/vertical coupling and beam distortions

We were able to observe beam distortions and horizontal/vertical coupling on the view screen behind the filter if we deliberately allowed for large deviations from the reference beam trajectory (>3 mm, >5 mm) at the input. This was technically feasible because the input collimator can be moved reproducibly in and out of the line by a pneumatic drive. Normally, the beam is confined to the reference axis to less than 1 mm at the input of the system. Trajectory calculations using field maps generated by TOSCA and CPO-3D show that even under this conditions coupling between the horizontal and vertical coordinates occurs. The field maps reveal the existence of the field components which lead to coupling, especially in the vicinity of the end plates.

The emittance measurements in Fig. 3 represent projections of the four dimensional beam space phase ellipsoid onto the x, x'- and y, y'-planes. Because of the couplings the area (i.e. the emittance) of these projections can change whereas the four-dimensional emittance remains unchanged. This effect may explain why we find an apparent growth of emittance with spin angle which amounts to 15% at $\Theta = \pi/2$ for the results in Fig. 3. In earlier measurements we have found even larger growth, probably because a stronger coupling was induced by a less careful alignment.

3.5. Influence of technical parameters

Two effects have been observed which have a certain influence on stability. The first is caused by the 10^{-4} ripple of the high voltage power supplies which leads to an observable (but tolerable) horizontal beam position fluctuation in the first microtron (few tenth of a mm) for the largest spin rotation angle.

The second effect is the drift (about 1 mm) of the beam position behind the filter during the first hour of operation when large angles are demanded. This is very likely due to temperature effects ($\Delta T = 40$ K of the filter body is observed due to heat dissipation from the magnetic coil) which can cause a thermal expansion of the field plates or by thermal drift of the power supplies. Again, the effect represents no problem since conditions remain stable after the transient time.

4. Operation of MAMI with the Wien-filter spin rotator

Fig. 5 presents the measured Mott scattering asymmetry at 3.5 MeV as a function of the spin rotation angle. Because the initial spin polarization is parallel to momentum, and because the Mott analyzing power has only a nonzero component perpendicular to the momentum, the observed asymmetry should behave like a sine wave without phase shift. The fit to our data supports this, e.g. the phase shift of the fit is only $\Phi = 0.003$ radian. The differences between the spin rotation angles calculated from the field distributions and the fit in Fig. 5 are less than 1%.

The close agreement of the measured points with the sinusoidal curve also indicates reproducibility of the rotation and of the measurement device. Similar curves have been observed with polarimeters behind the accelerator. It is evident that it is possible to achieve any desired spin orientation in the plane of the accelerator.

The filter has been used in several thousand hours of beam time. Particularly it has served for the experiments of the A4 collaboration at MAMI which are dedicated to the measurement of parity violating asymmetries. Their experiments have very stringent requirements concerning beam quality and stability which were met during these runs. In addition A4 required the spin orientation at the target to be frequently changed in the accelerator plane from parallel to perpendicular to the particle velocity [5,17]. Such a manipulation can now be achieved in less than one hour.

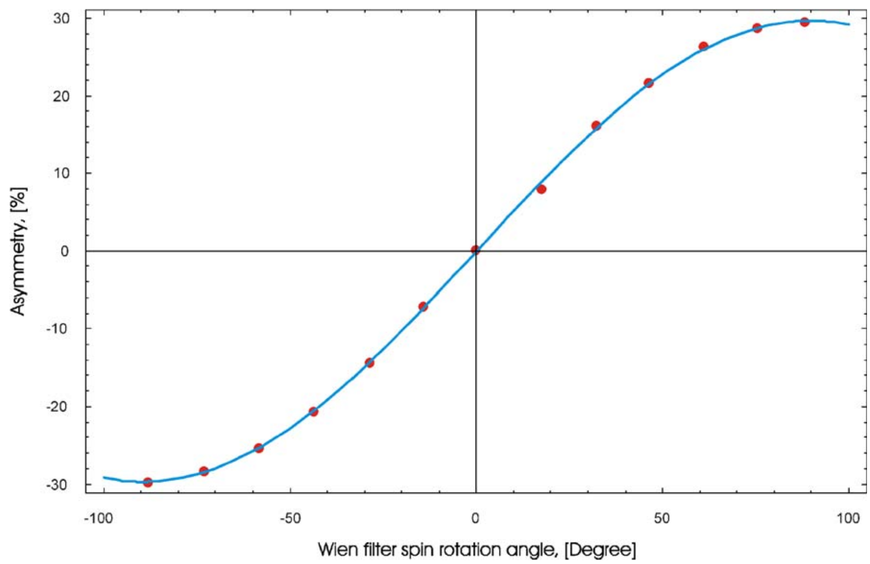

Fig. 5. Signal from the Mott-polarization monitor behind the 3.5 MeV injector of MAMI for different Wien-filter settings. Fit curve is A $(\Theta) = 0.296\sin(\Theta + \Phi)$. Statistical error bars are too small to be visible.

5. Conclusion

A Wien-filter spin rotation system was installed in the 100 keV injection beam line of MAMI. Several phenomena have been envisaged and observed which could in principle cause difficulties in operation. We have demonstrated that these effects can be kept well under control. First, the small beam emittance of the source of polarized electrons together with focusing the beam into the filter minimizes the effect of varying focal length in the accelerator plane to a tolerable level. Second, the shift of the central beam trajectory can be compensated with simple countermeasures. Nonlinearities and coupling between the x and y coordinates are in practice negligible.

The Wien system has been in operation since 2003 for run times adding up to several thousand hours without experiencing difficulties even for the most demanding experiments. Therefore the use of this device is foreseen as the standard spin tuning mechanism for the upcoming operation of MAMI-C.

Acknowledgments

The authors want to thank A. Jankowiak and E. Reichert for fruitful discussions during the preparation of this article. The support of the MAMI team during setting up the electron beam for the experiments presented here is especially acknowledged. This work was supported by the Deutsche Forschungsgemeinschaft within the framework of the Sonderforschungsbereich 443.

References

[1] H. Herminghaus, et al., Nucl. Instr. and Meth. 138 (1976) 1.
[2] K. Aulenbacher, et al., Nucl. Instr. and Meth. A 391 (1997) 498.
[3] D.I. Glazier, et al., Eur. Phys. J. A 24 (2005) 101.
[4] J. Ahrens, et al., Phys. Rev. Lett 87 (2001) 022003.
[5] F.E. Maas, et al., Phys. Rev. Lett. 93 (2004) 022002.
[6] L.H. Thomas, Phil. Mag. 3 (1927) 1.
[7] V. Bargman, et al., Phys. Rev. Lett. 2 (1959) 455.
[8] K.H. Steffens, et al., Nucl. Instr. and Meth. A 325 (1993) 378.
[9] V. Tioukine, et al., in: Proceedings of EPAC 2002, Paris, 2002, p. 1650.
[10] Ch. Prescott, private communication, 2004.
[11] M. Poelker, M. Farkondeh, private communication, 2004.
[12] M. Salomaa, H.A. Enge, Nucl. Instr. and Meth. 145 (1977) 279.
[13] D. Rubin, U. Cornell, Measurement and diagnosis of coupling and solenoid compensation, in: A.W. Chao, M. Tigner (Eds.), Handbook of Accelerator Physics and Engineering, World Scientific, Singapore, 1998.
[14] K. Brown, Single element optic, in: A.W. Chao, M. Tigner (Eds.), Handbook of Accelerator Physics and Engineering, World Scientific, Singapore, 1998.
[15] T. Roser, Spin rotation and Siberian snakes, in: A.W. Chao, M. Tigner (Eds.), Handbook of Accelerator Physics and Engineering, World Scientific, Singapore, 1998.
[16] J.T. Seeman, Transverse and longitudinal emittance measurements, in: A.W. Chao, M. Tigner (Eds.), Handbook of Accelerator Physics and Engineering, World Scientific, Singapore, 1998.
[17] F.E. Maas, et al., Phys. Rev. Lett. 94 (2005) 082001.